Dwarf Galaxies: From the Deep Universe to the Present
Proceedings IAU Symposium No. 344, 2019
K. B. W. McQuinn & S. Stierwalt, eds.

doi:10.1017/S1743921318005203

The merger debris of dwarf galaxies in the local stellar halo

Cuihua Du[1], Hefan Li[2] and Heidi Jo Newberg[3]

[1]College of Astronomy and Space Sciences, University of Chinese Academy of Sciences, Beijing 100049, China
email: ducuihua@ucas.ac.cn

[2]School of Physical Sciences, University of Chinese Academy of Sciences, Beijing 100049, China

[3]Department of Physics, Applied Physics and Astronomy, Rensselaer Polytechnic Institute, Troy, NY 12180, USA

Abstract. Based on the second Gaia data release and spectroscopy from the Large Sky Area Multi-Object Fiber Spectroscopic Telescope (LAMOST) Data, we identified 23,582 halo stars kinematically. The halo streams in the solar neighborhood could be detected in the space of energy and angular momentum. We reshuffle the velocities of these stars to determine the significance of the substructure. Finally, we find 14 statistically significant substructures and several substructures are not reported by previous works. These structures may be the debris of dwarf galaxies accretion event and their dynamical and chemical information can help to understand the history of the Galaxy.

Keywords. Galaxy: kinematics and dynamics - Galaxy: halo - Solar neighborhood

1. Introduction

In the standard hierarchical model of galaxy formation, the halos of galaxies like the Milky Way, are thought to form hierarchically via the accumulation of stars from dwarf galaxies and this merging process left behind many stellar streams and substructures in the Galactic halo. Although the accumulated debris from old accretion events rapidly disperses in space, a significant amount of recognizable substructure should be visible both spatially and in phase-space distribution. Numerical simulations predict that most accreted satellites would spread their tidal debris into the Galactic inner halo (Helmi, A. & White, S. D. M. 1999), thus we can expect to find debris remnants in the local halo. Some efforts have been made to find the debris relics in the local halo and the observational evidence is slowly growing. For example, Helmi *et al.* (1999b) have detected two streams in the solar neighborhood by studying the angular momentum of stellar orbits. Smith *et al.* (2009) found four discrete overdensities localized in angular momentum in the solar neighborhood and suggested that they may be possible accretion remnants. Kepley *et al.* (2007) assembled a sample of halo stars in the solar neighborhood to find two new halo substructure in velocity and angular momentum space. Recently, Helmi *et al.* (2017) use the TGAS dataset and RAVE survey to study the distribution of local halo stars in “Integrals of Motion” space and discover several substructures that could potentially be related to merger events. Although no longer spatially coherent, such stellar streams keep their common origin imprinted into their chemical and dynamical properties. This allows us constrain various scenarios of hierarchical buildup of the Galaxy from the phase-space distribution of local halo stars.

The chemical evolution of stellar halos, supports the idea that the outer halo formed primarily through the accretion of smaller stellar systems like dwarf spheroidal (dSph) galaxies (Searle & Zinn 1978; Springel *et al.* 2008; Klypin *et al.* 2011). On the other hand, part of the inner halo may have formed in-situ, either from dissipative collapse of gaseous material onto the central region of the Galaxy (Eggen *et al.* 1962; Zolotov *et al.* 2010; Font *et al.* 2011), or from a heated disk during merger events (Cooper *et al.* 2015). It is possible that the inner-halo was also built by accretion. In this work, based on the second Gaia data and LAMOST data, we can obtain the full 6D phase space information for halo stars to search substructures in the solar neighborhood.

2. Data

The second Gaia data (Gaia DR2) was released in April, 2018 and it includes high-precision measurements of nearly 1.7 billion stars Gaia Collaboration (2018). This data set contains positions, parallaxes, and mean proper motions for about 1.3 billion of the brightest stars. For a subset of stars within a few thousand parsec of the Sun, Gaia has measured the velocity in all three dimensions.

The LAMOST is a 4 meter quasi-meridian reflective Schmidt telescope with 4000 fibers within a field of view of 5°. The LAMOST spectrograph has a resolution of R $\sim$ 1,800 and wavelength range spanning 3,700 Å to 9,000 Å (Cui *et al.* 2012; Zhao *et al.* 2012). The survey reaches a limiting magnitude of $r = 17.8$ (where r denotes magnitude in the SDSS r-band), but most targets are brighter than $r \sim 17$.

Our initial sample was obtained by cross-matching between the Gaia and LAMOST catalogs. Considering the relative parallax error $\leqslant 20\%$, signal-to-noise ration (SNR) $\geqslant 20$, and radial velocity error $\epsilon_{RV} \leqslant$ 10 km/s, the sample is 2,583,106 objects. To get full 6D phase-space information, we invert the parallax to obtain distance. These star's Galactic space-velocity components U, V, and W can be derived.

3. Analysis method

Assuming the space velocities of the stellar populations in the thin-disk, the thick-disk, and the halo have Gaussian distributions, we can get the probability that a given star belongs to a specific population. At first, we use the SCI-KIT LEARN package in PYTHON (Pedregosa *et al.* 2012) to fit a two component Gaussian Mixture Model to the spherical velocities of the stars v_R, v_ϕ and v_z. The velocity dispersions are $(\sigma_R, \sigma_\phi, \sigma_z) = (64, 42, 42)$ km/s for thin disk and $(\sigma_R, \sigma_\phi, \sigma_z) = (35, 22, 18)$ km/s for think disk. The center of v_R and v_z are close to 0 km/s for both thin and thick disk. The center of v_ϕ is -222 km/s for thin disk and -181 km/s for think disk. By adopting the velocity ellipsoid $(\sigma_r, \sigma_\theta, \sigma_\phi) = (141, 75, 85)$ km/s and mean rotation ($\mu_\phi = -38.8$ km/s) of halo stars from Bond *et al.* (2010), we can get the probability of stellar halo (H) in spherical coordinate. Then we can get two relative probabilities for the halo-to-thin-disk (H/D) and halo-to-thick-disk (H/TD) for each star in our sample. We selected halo stars with H/D > 60 and H/TD > 60. The final sample has 23,582 stars.

We now search local stellar halo substructures in this sample halo stars. For each star in our halo sample, we compute the energy and angular momentum by adopting a Galaxy potential model provided by McMillan (2017). In order to constrain our sample in populated region, we select these stars within $-1600 < L_z < 2300$ km/s kpc, $-2.1 \times 10^5 < E < -0.7 \times 10^5$ km^2/s^2, and $L_\perp < 2600$ km/s kpc. We apply the SCI-KIT LEARN implementation of a non-parametric density estimator to determine the density field of the stars in $E - L_z - L_\perp$ space. The data is scaled to unit variance.

To investigate the probability that any substructure in the real data may happen by chance, we reshuffle velocities 6000 times to create randomized datasets. We recompute

https://doi.org/10.1017/S1743921318005203 Published online by Cambridge University Press

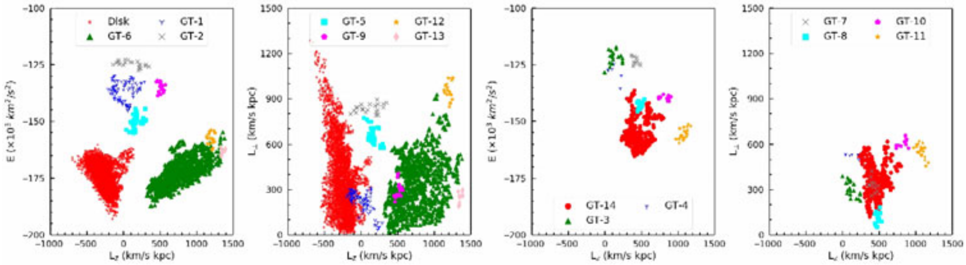

Figure 1. Distribution in $E - L_z - L_\perp$ space, for the stars comprising the identified substructures and disk.

their distribution in $E - L_z - L_\perp$ space and use the kernel density estimator with same parameters to get the density. For each pixel in $E - L_z - L_\perp$ space, we count the frequency of the randomized data larger than the real data and mark where the count less than 20 temporarily. When we perform a similar analysis using one of the random datasets as the real data, we notice that there are also some overdensities. It indicates that the overdensities identified in the real data are probably produced by chance. Smaller structures (small size or low density) are more likely produced by chance. So we change these parameters to ensure that no substructure appears in 600 random datasets.

Finally, we identidied 15 statistical overdensities in "Integrals of Motion" space and they are shown in Figure 1. Our halo sample contains some possible thick disk stars, and these stars concentrate in the prograde and high binding energy region. One overdensity may belong to the think disk, because the member stars in this substructure locate at the above region and they have highly TD/H and metallicity. We label the substructures GT-1 through 14.

We compare our substructures with other reported substructures (e.g. Klement *et al.* 2009). The substructure GL-14 identified in our sample and "Kapteyn" stream Eggen (1996) have similar ν, V_{az} and $V_{\Delta E}$. The GL-8 identified in this work is smilar to "C2" stream in Klement *et al.* (2009), and the distributions of the part of GL-6 in our sample are similar to VelHel-5 of Helmi *et al.* (2017). It is possible that these streams related to each other, and could originate from the same population. Li *et al.* (2017) present the candidate members of the Pal 5, GD-1, Cetus Polar and Orphan tidal stellar streams found in LAMOST DR3, SDSS DR9 and APOGEE catalogs. But we found no overlap between their stellar streams and our substructures. Liang *et al.* (2017) applied the wavelet transform method to detect 16 significant overdensities in velocity space. Due to the sample election effects, those stellar streams found in other surveys are not included completely in our cross-matched set.

4. Conclusions

By cross-matching the Gaia DR2 and LAMOST DR5 data, we obtain a sample of stars with full phase-space information and identified sample halo stars kinematically. Our final halo sample consists of 23,582 stars. We determine the distribution of the sample halo stars in "Integrals-of-Motion" space, defined by two components of the angular momentum, $L_\perp$ and L_z, and by energy. To remove the contamination, we estimate the statistical significance for these overdensities and identify 15 overdensities. Of these overdensities, one seems to be associated to the metal-poor tail of thick disk due to the velocities and metallicity of prograde stars. Three substructures may correspond to the "Kapteyn" stream of Eggen (1996), C2 of Klement *et al.* (2009) and VelHel-5 of Helmi *et al.* (2017). Eleven substructures are not reported in previous works. The identified structures may be the debris from satellite accretion events and their dynamical and chemical properties can aid in understanding the history of the Milky Way.

Acknowledgements

This work has made use of data from the European Space Agency (ESA) mission Gaia (http://www.cosmos.esa.int/gaia), processed by the Gaia Data Processing and Analysis Consortium (DPAC, http://www.cosmos.esa.int/web/gaia/dpac/consortium). Funding for DPAC has been provided by national institutions, in particular the institutions participating in the Gaia Multilateral Agreement. The Guoshoujing Telescope (LAMOST) is a National Major Scientific Project has been provided by the National Development and Reform Commission. LAMOST is operated and managed by the National Astronomical Observatories, Chinese Academy of Sciences. This work was supported by joint funding for Astronomy by the National Natural Science Foundation of China and the Chinese Academy of Science, under Grants U1231113. This work was also by supported by the Special funds of cooperation between the Institute and the University of the Chinese Academy of Sciences, and China Scholarship Council (CSC).

References

Bland-Hawthorn, J., & Gerhard, O. 2016, *ARAA*, 54, 529
Bond, N. A., Ivezić, Ž, Sesar, B., *et al.* 2010, *ApJ*, 716, 1
Cooper A. P., Parry O. H., Lowing B., *et al.* 2015, *MNRAS*, 454, 3185
Cui X.-Q., Zhao Y.-H., Chu Y.-Q., *et al.* 2012, *RAA*, 12, 1197
Eggen, O. J. 1996, *AJ*, 112, 1595
Eggen, O. J., Lynden-Bell, D., & Sandage, A. R. 1962, *ApJ*, 136, 748
Font, A. S., Mccarthy, I. G., Crain, R. A., *et al.* 2011, *MNRAS*, 416, 2802
Gaia Collaboration, (Brown, A. G. A., *et al.*) 2018, arXiv:1804.09365
Helmi, A., & White, S. D. M. 1999a, *MNRAS*, 307, 495
Helmi, A., White S. D. M., de Zeeuw P. T., *et al.* 1999b, *Nature*, 402, 53
Helmi, A., Veljanoski J., Breddels M. A., *et al.* 2017, *A&A* , 598, A58
Kepley, A. A., Morrison, H. L., Helmi, A., *et al.* 2007, *AJ*, 134, 1579
Klement, R., Rix, H. W, Flynn, C., *et al.* 2009, *ApJ*, 698, 865
Klypin, A. A., Trujillo-Gomez, S., & Primack, J. 2011, *ApJ*, 740, 102
Li, G.-W., Yanny, B., Zhang, H.-T., *et al.* 2017, *RAA*, 17, 62
Liang, X.-L., Zhao, J.-K., Oswalt, T. D., *et al.*, 2017, *ApJ*, 844, 152
McMillan, P. J. 2017, *MNRAS*, 465, 76
Pedregosa, F., Varoquaux, G., Gramfort, A., *et al.* 2012, arXiv:1201.0490
Searle, L., & Zinn, R. 1978, *ApJ*, 225, 357
Smith, M. C., Evans, N. W., Belokurov, V., *et al.* 2009, *MNRAS*, 399, 1223
Springel, V., Wang, J., Vogelsberger, M., *et al.* 2008, *MNRAS*, 391, 1685
Zolotov, A., Willman, B., Brooks, A., *et al.* 2010, *ApJ*, 721, 738
Zhao, G., Zhao, Y.-H., Chu, Y.-Q., *et al.* 2012, *RAA*, 12, 723

Discussion

Q1. What is the contribution brought by LAMOST data to the analysis presented here?

A1. We use the metallicity and radial velocity provided by LAMOST.